nature cell biology

An organized and functional thymus generated from FOXN1-reprogrammed fibroblasts

Nicholas Bredenkamp[1,3], Svetlana Ulyanchenko[1], Kathy Emma O'Neill[1], Nancy Ruth Manley[2], Harsh Jayesh Vaidya[1] and Catherine Clare Blackburn[1,4]

A central goal of regenerative medicine is to generate transplantable organs from cells derived or expanded *in vitro*. Although numerous studies have demonstrated the production of defined cell types *in vitro*[1], the creation of a fully intact organ has not been reported. The transcription factor forkhead box N1 (FOXN1) is critically required for development of thymic epithelial cells[2,3] (TECs), a key cell type of the thymic stroma[4]. Here, we show that enforced *Foxn1* expression is sufficient to reprogramme fibroblasts into functional TECs, an unrelated cell type across a germ-layer boundary. These FOXN1-induced TECs (iTECs) supported efficient development of both CD4$^+$ and CD8$^+$ T cells *in vitro*. On transplantation, iTECs established a complete, fully organized and functional thymus, that contained all of the TEC subtypes required to support T-cell differentiation and populated the recipient immune system with T cells. iTECs thus demonstrate that cellular reprogramming approaches can be used to generate an entire organ, and open the possibility of widespread use of thymus transplantation to boost immune function in patients.

The thymus, the primary lymphoid organ crucially required for generation of a functional T-cell repertoire[5], is the first organ to degenerate during normal ageing, a process termed age-related thymic involution (thymic involution herein)[6]. Thymic involution is a critical factor in the impaired capacity of adult patients to recover adaptive immunity following therapeutic immune depletion[7]. Thus, development of improved thymus-based therapies for enhancing immune system function in patients is of broad interest. TECs are critical effectors in the intrathymic microenvironments required for T-cell development. Two distinct TEC sublineages exist, located in the cortical and medullary compartments of the thymus[8]. These cortical (c) and medullary (m) TECs mediate discrete aspects of T-cell development, and their segregation into distinct compartments is thought vital for accurate and efficient production of a self-restricted, self-tolerant T-cell repertoire. Despite their functional differences, cTEC and mTEC initially arise from a common progenitor TEC, and the forkhead transcription factor FOXN1, expressed exclusively in thymic and cutaneous epithelia, is required at multiple stages for differentiation of both sublineages[2,3,9,10]. Neonatal thymus transplantation can confer adaptive immunity to congenitally athymic patients[11] but its widespread use is limited by donor tissue supply and histocompatibility; these limitations would be overcome if functional TECs could be generated or expanded *in vitro*. Several investigators have reported derivation of TEC-like cells from pluripotent cells by directed differentiation using growth factors[12–16]; however, neither generation from these TEC-like cells of an organized thymus containing all TEC subtypes, nor their capacity to support T-cell development *in vitro* has been demonstrated. Although in one report TECs expressing the transcription factor autoimmune regulator (AIRE), which are critical for the establishment of self-tolerance[17], were detected after transplantation of the pluripotent cell-derived TECs, there, no demarcation of cortical and medullary compartments was evident[16]. In sum, the challenge of generating therapeutically useful TECs *in vitro* that can form a fully functional thymus on transplantation remains unsolved. Here, we have examined two questions: first, whether the alternative approach of direct reprogramming can be used to generate functional TECs *in vitro*, and second, whether artificial TECs derived by this method can generate a complete thymus on transplantation.

To address the first question, we tested the outcome of enforcing expression of FOXN1, our candidate reprogramming factor, in primary mouse embryonic fibroblasts (MEFs). For this purpose, we developed a transgenic mouse line in which a full-length *Foxn1* complementary DNA under the control of the *CAG* promoter was knocked into the *Rosa26* locus, with a LoxP-flanked transcriptional STOP cassette inserted between the *CAG* promoter and the *Foxn1* cDNA (*Rosa26*$^{CAG-STOP-Foxn1-IRES-GFP}$;

[1]Medical Research Council Centre for Regenerative Medicine, Institute for Stem Cell Research, School of Biological Sciences, University of Edinburgh, SCRM Building, 5 Little France Drive, Edinburgh EH16 4UU, UK. [2]Department of Genetics, University of Georgia, Athens, Georgia 30602, USA. [3]Present address: Wellcome Trust-MRC Stem Cell Institute, University of Cambridge, Tennis Court Road, Cambridge CB2 1QR, UK.
[4]Correspondence should be addressed to C.C.B. (e-mail: c.blackburn@ed.ac.uk)

Received 16 December 2013; accepted 10 July 2014; published online 24 August 2014; DOI: 10.1038/ncb3023

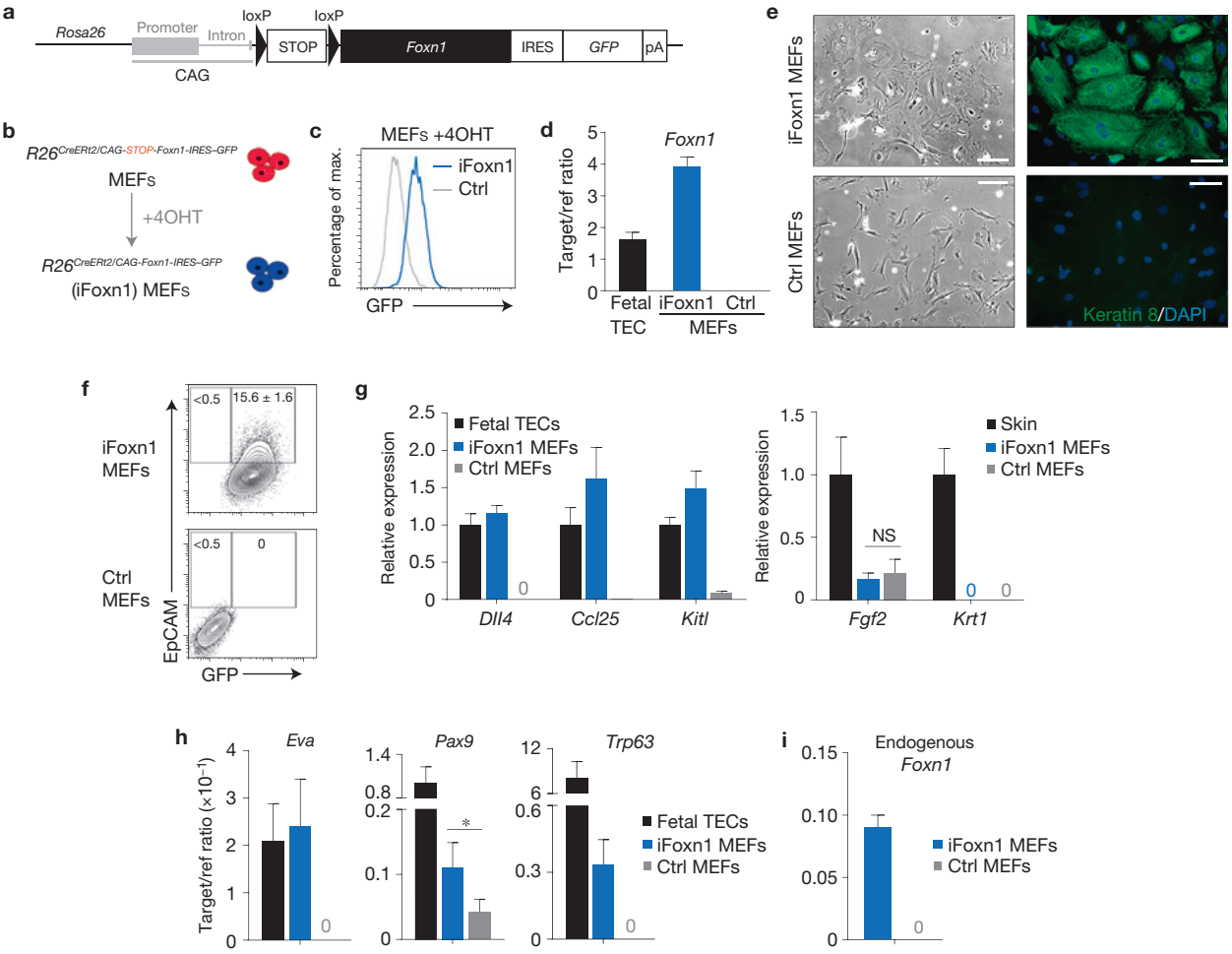

Figure 1 Enforced FOXN1 expression induces epithelial identity in fibroblasts. (**a**) iFoxn1 transgene. (**b**) Schematic showing the procedure for generating iFoxn1 MEFs. (**c**) GFP expression in iFoxn1 and *Rosa26*$^{CreERt2/+}$ (control) MEFs 10 days after 4-hydroxy tamoxifen (4OHT) treatment. (**d**) *Foxn1* mRNA expression in iFoxn1 and *Rosa26*$^{CreERt2/+}$ control MEFs 10 days after 4OHT treatment, and E15.5 wild-type EpCAM^{+} fetal TEC, normalized to the geometric mean of two housekeeping genes. Data shown are mean ± s.d. from $n=3$ independent experiments. (**e**) Bright-field (left) and immunofluorescence images (right) showing morphology and K8 staining, 10 days after 4OHT treatment. Scale bars, 100 μm. (**f**) EpCAM and GFP expression 10 days after 4OHT treatment, after gating on live cells. Values shown are mean ± s.d. from $n=3$ independent experiments. (**g**–**i**) mRNA expression levels of the genes shown in purified EpCAM^{+} iFoxn1 and control MEFs normalized to the geometric mean of two housekeeping genes. Data shown are mean ± s.d. from $n=3$ independent experiments (NS, not significant; $^{*}P<0.05$). In **g**, expression level is shown relative to E15.5 EpCAM^{+} fetal TEC or skin. In **d**,**g**–**i**, blue bars, *Rosa26*$^{CreERt2/CAG-Foxn1-IRES-GFP}$ (iFoxn1); grey bars, *Rosa26*$^{CreERt2/+}$ (control); black bars, fetal TEC, except right hand panel in **g**, where black bars represent skin. For **c**–**i** $n\geq 3$ independent experiments. Three technical replicates were run for each *n*. cDNA was generated from 200 cells using a one-step RT-qPCR method with amplification (**d**,**g**,**h**) or from 50,000 cells without amplification (**i**). Error bars or values show mean ± s.d. Ctrl, control. See also Supplementary Figs 1 and 2.

Fig. 1a and Supplementary Fig. 1). Crossing with *Rosa26*^{CreERt2} mice generated *Rosa26*$^{CreERt2/CAG-STOP-Foxn1-IRES-GFP}$ embryos, from which we derived primary MEFs. Tamoxifen-induced Cre-mediated excision of the STOP cassette in these MEFs generated *Rosa26*$^{CreERt2/CAG-Foxn1-IRES-GFP}$ (iFoxn1) MEFs, in which *Foxn1* expression was induced at levels comparable to fetal TECs (Fig. 1b–d); tamoxifen-independent Cre-mediated excision was not detected (Supplementary Fig. 2).

By ten days after initiation of *Foxn1* expression, the morphology of iFoxn1 MEFs had changed from an elongated, bipolar shape characteristic of fibroblasts, to a broader, polygonal shape, characteristic of epithelial cells (Fig. 1e). The identity of these cells was probed using the epithelial-specific markers keratin 8 (K8) and epithelial cell adhesion molecule (EpCAM), which are expressed by all TECs during early thymus development[9,18]. Most, if not all, iFoxn1 MEFs, but no control MEFs, expressed K8 (Fig. 1e), and approximately 15% expressed EpCAM (Fig. 1f), suggesting that FOXN1 induction had converted the fibroblasts to an epithelial-like state.

To investigate the identity of the epithelial-like iFoxn1 MEFs, we isolated EpCAM^{+} cells and analysed them for expression of TEC- (*Dll4*, *Ccl25* and *Kitl*; refs 9,19) and cutaneous epithelium- (*Fgf2* and *Krt1*; ref. 20) specific FOXN1-regulated genes. The iFoxn1 MEFs but not control MEFs expressed *Dll4*, *Ccl25* and *Kitl* at levels comparable to fetal TECs, but did not express cutaneous epithelium-associated genes (Fig. 1g). Other TEC-associated genes not previously implicated as FOXN1 targets, *Epithelial V-like antigen (Eva or Mpzl2)*, which

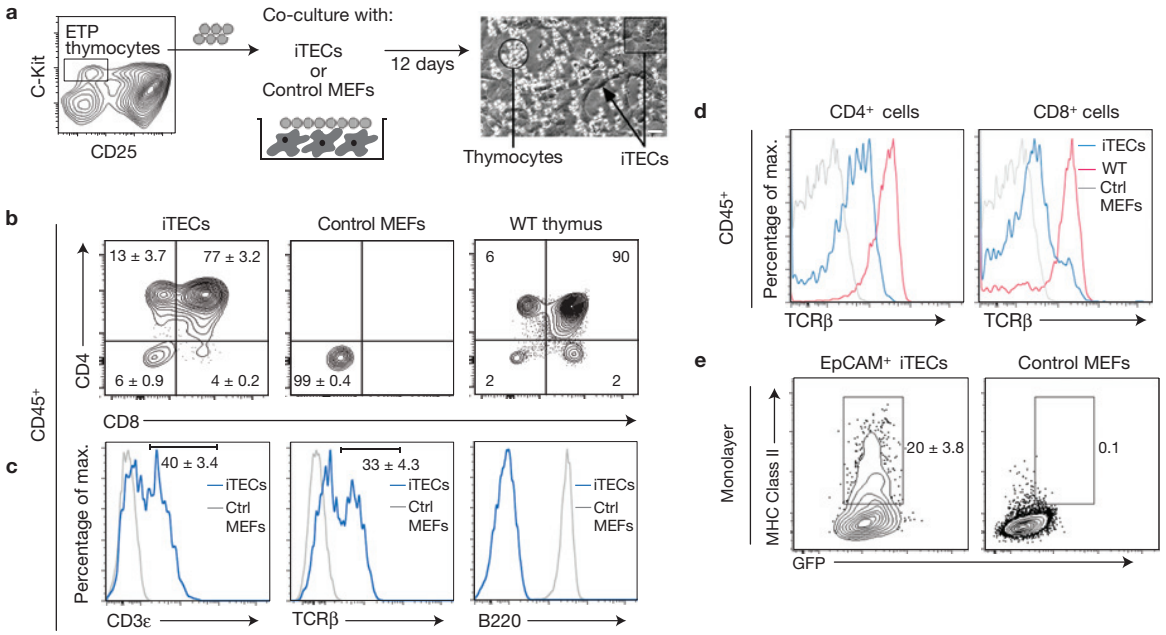

Figure 2 iTECs can support T-cell development *in vitro*. (**a**) Strategy for *in vitro* T-cell differentiation assay. Monolayers of iTECs or control MEFs, 7 days following 4-hydroxy tamoxifen (4OHT) treatment, were seeded with ETP ($Lin^-CD25^-C\text{-}Kit^+$) isolated from E14.5 wild-type thymus lobes and were analysed 12 days later (Lin: CD3ε, CD4, CD8, CD11b, CD11c, B220, Gr-1, NK1.1, Ter119). Right panel, bright-field image of iTEC/thymocyte co-culture. Scale bar, 50 μm. (**b**–**d**) Plots show staining after gating on $CD45^+$ cells following 12 days of co-culture with iTECs or control MEFs. Values shown are mean ± s.d. from $n=4$ independent experiments. WT, wild type. (**d**) TCRβ expression on $CD4^+$ and $CD8^+$ cells from iTEC co-cultures or wild-type thymus. (**e**) Control MEFs or iTECs after gating on $CD45^-$ cells, and $EpCAM^+$ cells for iTECs, following 12 days of co-culture with thymocytes. Values shown are mean ± s.d. from $n=3$ independent experiments. See also Supplementary Figs 3 and 4.

is broadly expressed in TECs, and *Pax9* and *Trp63* (ref. 19), which are differentially expressed among TEC subsets, were also induced in iFoxn1 MEFs (Fig. 1h). We consistently detected low levels of endogenous *Foxn1* (Fig. 1i), indicating a direct auto-regulatory mechanism and/or indirect activation of endogenous *Foxn1* as part of an initiated TEC differentiation programme. Collectively, enforced FOXN1 expression in MEFs induces genes involved in TEC development and function, suggesting a FOXN1-mediated conversion of MEFs into TEC-like cells (designated iTECs hereafter). FOXN1 is also expressed in cutaneous epithelium, yet here clearly induces a transcriptional programme characteristic of TECs rather than cutaneous epithelium. Although the reasons for this are not understood, the gene expression programme in TECs clearly shares some elements with that of cutaneous epithelium (p63, keratins, some claudins). This may relate to the high levels of FOXN1 induced in our system, and to the intracellular context provided by the iTEC-induction protocol.

To test the functional attributes of the iTECs, we determined their capacity to support T-cell development *in vitro*. A monolayer of iTECs, in which FOXN1 had been induced for seven days, was seeded with fetal $Lin^-CD25^-C\text{-}Kit^+$ early T lineage progenitors[21] (ETPs). Analysis after 12 days of co-culture (Fig. 2a) revealed the presence of $CD4^+CD8^+$ double-positive ($CD4^+CD8^+$ DP), $CD4^+$ single-positive ($CD4^+$ SP) and $CD8^+$ single-positive ($CD8^+$ SP) cells, with the subset distribution on the iTEC monolayers closely resembling that of the adult mouse thymus (Fig. 2b). As expected, the T cells generated on the iTEC monolayer expressed both CD3ε and T-cell antigen receptor beta (TCRβ; Fig. 2c,d). In contrast, ETPs seeded onto control MEFs did not enter thymopoiesis (Fig. 2b); instead, most haematopoietic cells remaining after co-culture on MEFs expressed the B-cell marker B220 (Fig. 2c). Consistent with the requirement for MHC Class II on TECs for positive selection and therefore efficient generation of $CD4^+$ SP thymocytes, $EpCAM^+$ iTECs showed robust expression of MHC Class II after co-culture with thymocytes (Fig. 2e). Surface MHC Class II was not evident in iTECs before co-culture, demonstrating that the cells generated by the initial reprogramming step differentiated on exposure to developing T cells, as observed for TECs within the native thymus *in vivo*[22]. Interestingly, the capacity of iTECs to support thymocyte development was dependent on their plating density, with a high density (>500 cells mm^{-2}) producing >3 times more $CD4^+CD8^+$ T cells within 12 days than a lower density (<250 cells mm^{-2}; Supplementary Fig. 3). However, the addition of fibroblast growth factor 7 (FGF7; ref. 23) to low-density iTECs substantially improved their ability to support T-cell development (Supplementary Fig. 3), consistent with the established role of FGF7 as a mitogen for fetal and postnatal TECs (ref. 23). Of note, FGF7 does not affect fibroblast proliferation[24], and FgfR2IIIb, the receptor for FGF7 and FGF10, is required for normal thymus development[23]. The kinetics of T-cell development were similar when ETPs were seeded onto iTECs or the stromal cell line OP9-DL1 (Supplementary Fig. 4), although as expected, development of $CD4^+$ SP thymocytes was typically more efficient in iTEC cultures (Supplementary Fig. 4). Collectively, iTECs can robustly support T-cell development *in vitro*, with thymocyte differentiation to the $CD4^+$ and $CD8^+$ SP stages closely mirroring *in vivo* differentiation. Although further work is required to test the capacity of iTECs to support T-cell development from the circulating lympho-myeloid proliferating progenitor, which is considered to

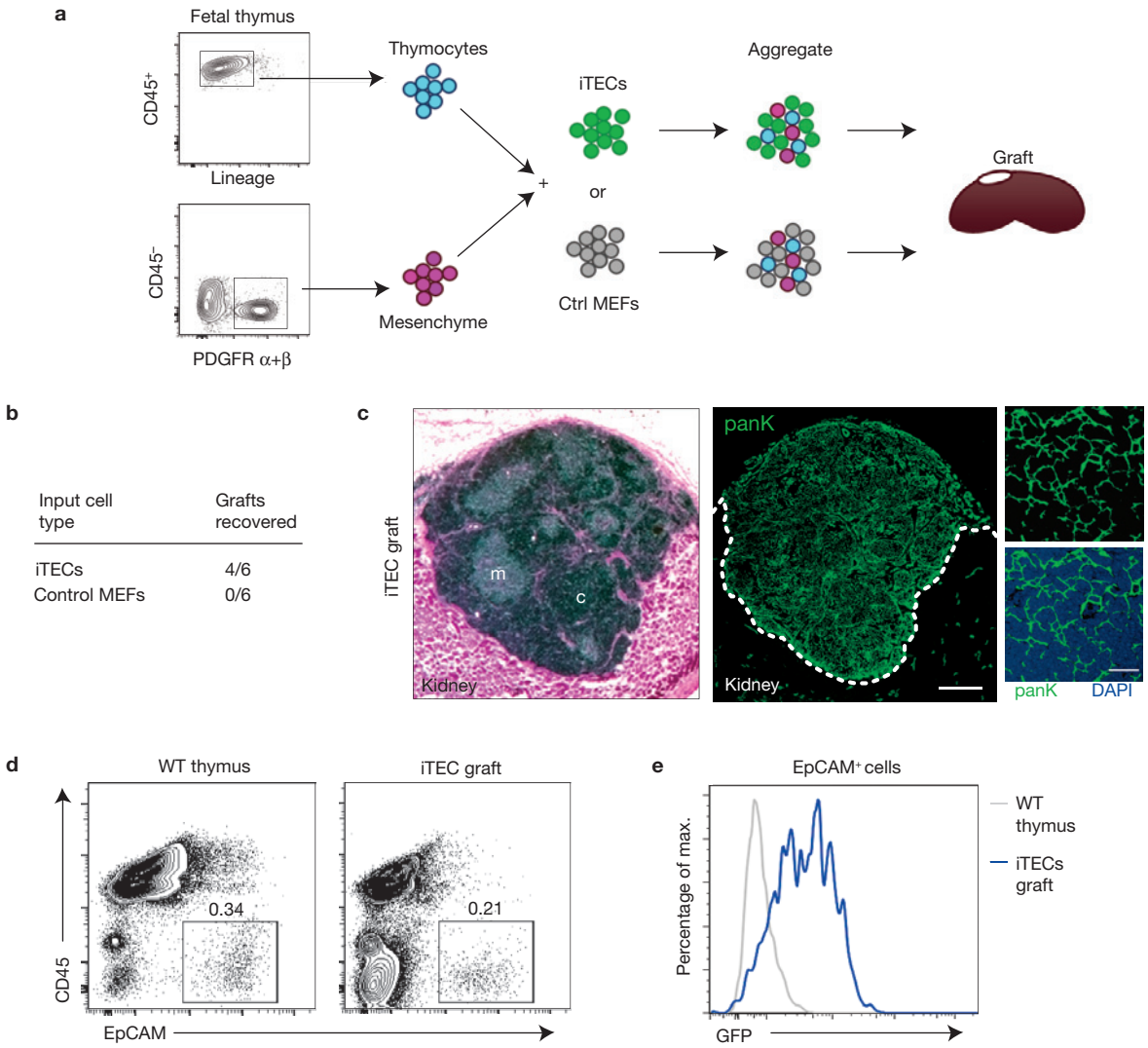

Figure 3 iTEC form a functional thymus *in vivo*. (**a**) Schematic of grafting assay. iTECs (5 days following FOXN1 induction) or control MEFs were aggregated with E12.5–13.5 wild-type CD45$^+$Lin$^-$ thymocytes and E12.5–13.5 wild-type CD45$^-$PDGFRαβ$^+$ thymic mesenchymal cells, and grafted under the kidney capsule of adult mice. Lin: CD3ε, CD4, CD8, CD11b, CD11c, B220, Gr-1, NK1.1, Ter119. (**b**) Summary of recovered grafts. (**c**) Haematoxylin and eosin staining (left), and pan-cytokeratin (panK; right) staining of an iTEC-derived kidney graft. m, medulla; c, cortex; scale bar, 500 μm. (**d**,**e**) Analysis of iTEC grafts, and wild-type (WT) thymi from 8-week-old mice. (**e**) CD45$^-$EpCAM$^+$ cells from the gate defined in **d**; GFP expression reports CAG–iFoxn1. Data shown are representative and are from 1 of at least 3 independent experiments.

be the thymus-seeding haematopoietic progenitor that gives rise to mature T cells[25,26], we anticipate that iTECs will have this capacity as it is well established that lympho-myeloid proliferating progenitors differentiate into T cells in co-culture with OP9-DL1 cells[25,27,28].

To address our second question, of whether the iTECs, an artificial cell type generated *in vitro*, could form an organized and functional thymus, we aggregated iTECs (5 days after induction of FOXN1) or control MEFs with immature thymocytes (CD45$^+$Lin$^-$) and fetal thymic mesenchyme from embryos at day 12.5 to 13.5 of development (E12.5–13.5) (CD45$^-$PDGFRαβ$^+$), and grafted the resulting cell aggregate under the kidney capsule of syngeneic adult mice[29,30] (Fig. 3a). Fetal thymic mesenchyme was included to ensure that growth factors essential for expansion of the thymus, including FGF10 and IGF (refs 23,31,32), were available within the graft. Macroscopic, well-formed organs were recovered 4 weeks post-grafting from recipients of iTEC, but not control MEF-only, grafts (Fig. 3b). These iTEC-derived organs exhibited a characteristic thymus morphology, with multiple clearly defined cortical and medullary regions evident in all grafts (Fig. 3c). Pan-cytokeratin staining revealed a reticular network of epithelial cells throughout the organs (Fig. 3c), while flow cytometric analysis indicated that haematopoietic and epithelial cells were present in similar proportions in the recovered iTEC grafts to in the native adult thymus (Fig. 3d). All EpCAM$^+$ cells in the iTEC grafts expressed GFP, reporting the transgenic iFoxn1–IRES–GFP messenger RNA, confirming they were derived from the input iTECs (Fig. 3e).

Thymus architecture and function are intimately linked, and furthermore, the presence of discrete TEC subsets within the cortical and medullary compartments is required for full functionality of the organ[9], including for inducing central tolerance in the emerging T-cell repertoire[33]. Correctly compartmentalized regions of cTECs

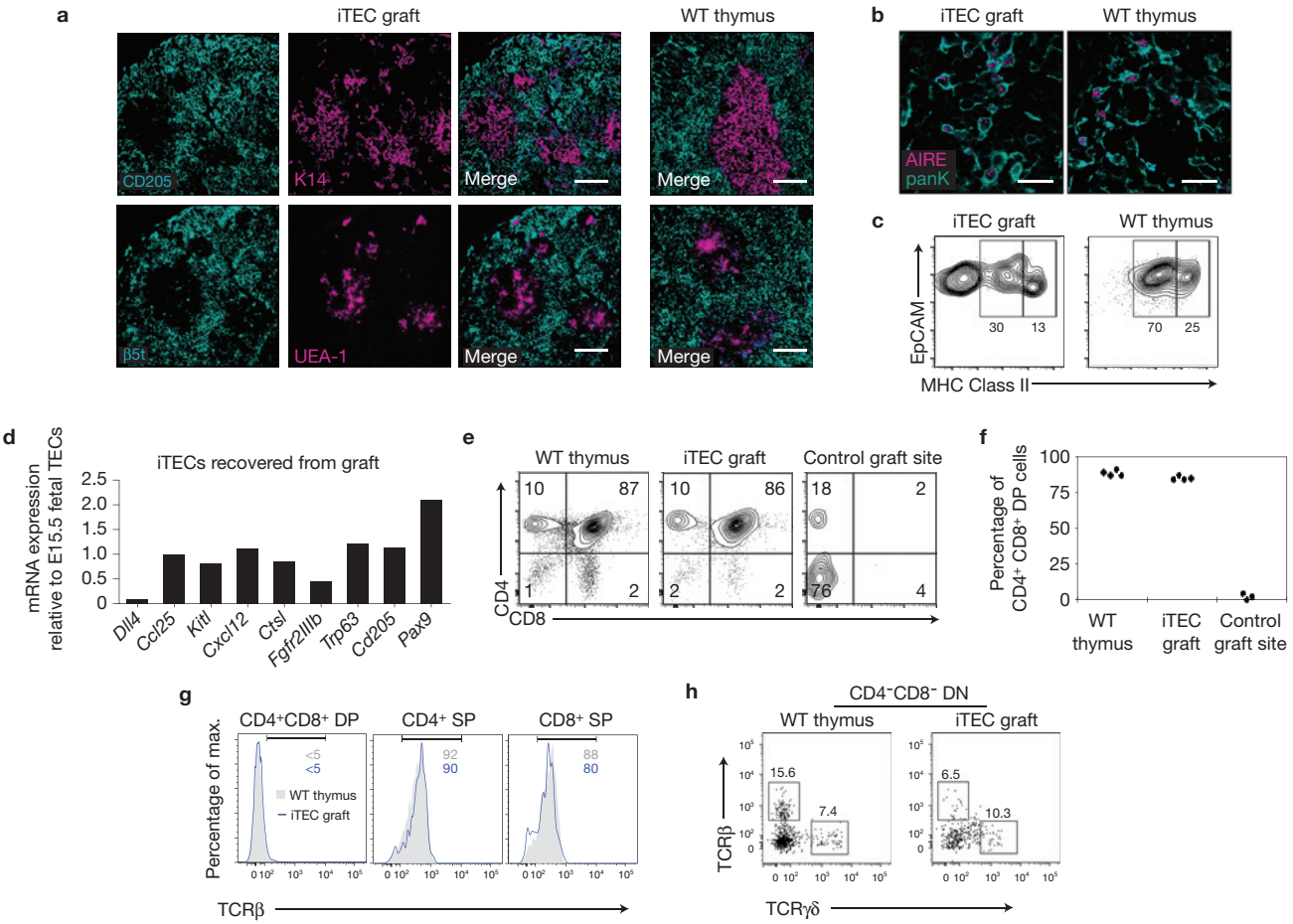

Figure 4 Intrathymic T-cell development in iTEC-derived grafts. (**a**,**b**) Immunohistochemical analyses of iTEC grafts and wild-type (WT) thymi using cTEC (CD205 and β5t) and mTEC (keratin 14 (K14) and UEA-1)-specific markers, and anti-AIRE. Scale bars: 150 μm (**a**), 25 μm (**b**). (**c**) Flow cytometry of MHC Class II expression for the CD45$^-$EpCAM$^+$ cells defined in Fig. 3d. Gates show MHC Class II^{lo} and MHC Class II^{hi} populations defined using wild-type TECs. In **a**–**c**, the data shown are representative and are from 1 of at least 4 independent experiments. (**d**) RT-qPCR analysis of 50 CD45$^+$EpCAM$^+$MHC Class II$^+$ iTECs, recovered from a single graft 7 weeks post-transplantation, for the markers shown. Data are shown relative to expression in E15.5 wild-type total EpCAM$^+$ TECs after normalization to two housekeeping genes (*Hmbs* and *Tbp*); expression level in E15.5 wild-type is 1 for all samples. Values shown are from 1 experiment. (**e**–**h**) Analysis of 8-week-old wild-type mouse thymus, iTEC grafts or cells collected from a control MEF graft site at 4 weeks post-transplantation. **f**–**h** show thymocyte populations defined in **e**. (**e**) CD4 and CD8 expression after gating on CD45$^+$ cells. (**f**) Percentage of CD4$^+$CD8$^+$ cells. (**g**) TCRβ expression. (**h**) TCRγδ expression on CD4$^-$CD8$^-$ thymocytes. In **e**,**g** data shown are representative and are from 1 of at least 4 independent experiments, in **f** each data point represents a separate graft from $n = 4$ independent experiments, and in **h** data shown are from 1 experiment.

and mTECs were evident in the iTEC-derived grafts, and expressed region-appropriate markers (CD205 and keratin 14 respectively[18,34]; Fig. 4a). The functional cTEC marker β5t (ref. 35), and the UEA-1^{hi} subpopulation of mTECs (ref. 9), were also evident (Fig. 4a). Functional competence was further demonstrated by the presence of AIRE$^+$ mTEC (ref. 33) and MHC Class II^{lo} and MHC Class II^{hi} TEC populations (Fig. 4b,c). iTECs recovered from the grafts expressed a range of markers associated with TEC differentiation and function at or close to the levels normally present in TECs (Fig. 4d). Thus, iTECs were able to differentiate to generate a functional thymus containing all of the major TEC populations and exhibiting the architectural characteristics diagnostic of a fully functional native thymus.

A crucial question was whether the iTEC-derived grafts supported normal T-cell development, and hence population of the peripheral immune system with newly generated naive T cells. Thymocyte subset distribution in the iTEC-derived grafts closely matched that of the native adult thymus (Fig. 4e,f). Distribution of TCRβ expression within iTEC grafts was near identical to that observed within the native thymus, with TCRβ^{hi} cells restricted to CD4$^+$ SP and CD8$^+$ SP populations (Fig. 4g). TCRγδ$^+$ T cells were present within CD4$^-$CD8$^-$ double-negative (DN) populations, again at a comparable proportion in the iTEC grafts and native thymus (Fig. 4h). No macroscopic grafts were recovered from MEF-graft recipients, and no evidence of thymopoiesis could be found in tissue adjacent to the graft site in any MEF-graft recipient mice (Fig. 4e,f). The T cells generated in the iTEC grafts were exported to populate the peripheral immune system. Peripheral blood analysis revealed the presence of CD4$^+$ and CD8$^+$ T cells, and Foxp3$^+$ regulatory T cells in two of three *nu/nu* iTEC recipient mice by 8 weeks post grafting, with numbers continuing to rise over time, whereas no donor-derived peripheral

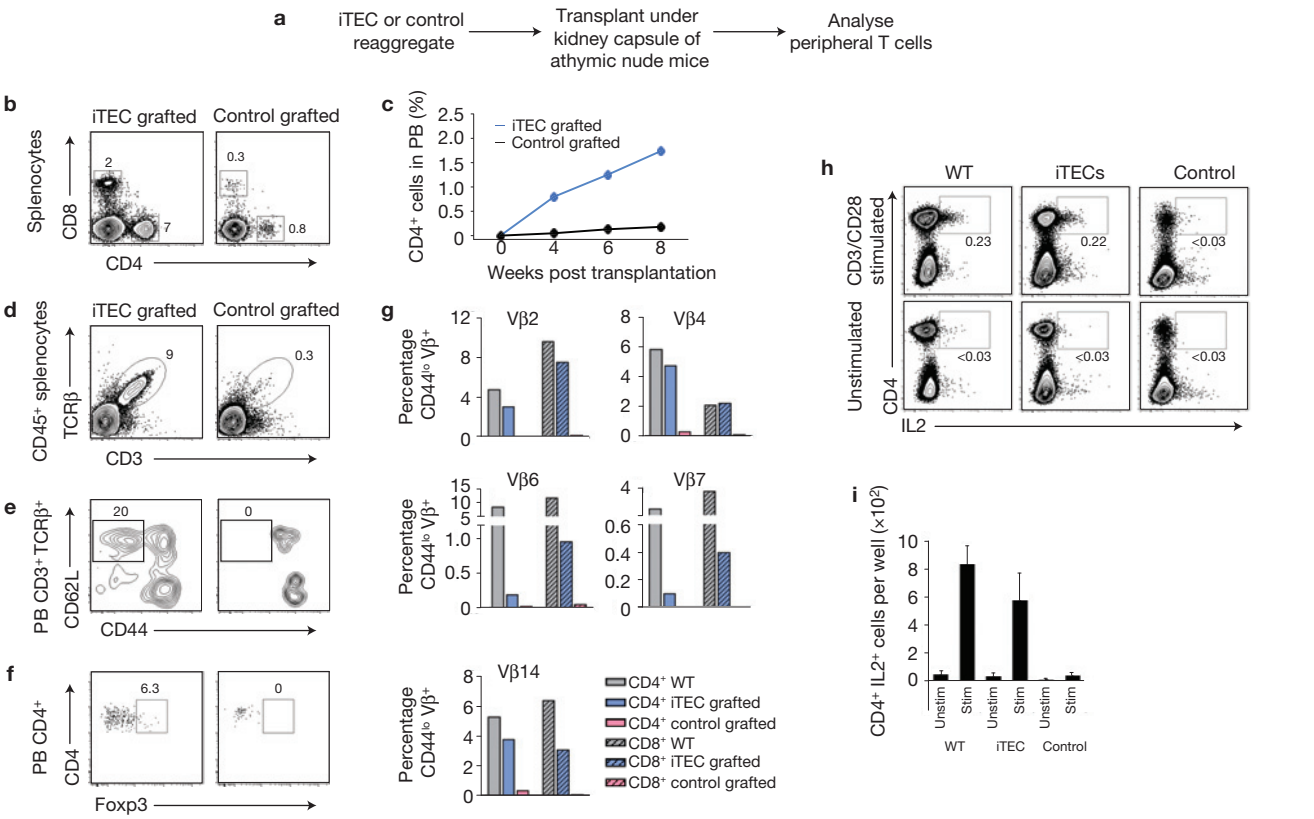

Figure 5 A diverse and functional peripheral T-cell repertoire is generated by iTEC-derived grafts. (**a**) Schematic showing the experimental design for **b**–**i**. (**b**–**f**) Representative analysis of spleen and lymph node cells or peripheral blood (PB) from nude mice, using the T-cell markers indicated. T cells were detected in the peripheral blood of two of three iTEC recipients. Splenocytes (**b**,**d**) or peripheral blood (**c**,**e**,**f**) from 6 weeks (**f**), 8 weeks (**e**), 14 weeks (**b**,**d**) or 2-weekly intervals, as shown (**c**), post-transplantation. In **b**,**d**,**e** data shown are representative and are from 1 of at least 3 independent experiments, and in **c** values shown are mean from $n=2$ independent experiments. Values used to derive mean in **c**: iTEC graft recipient mice at 0 weeks, 0; 4 weeks, 1.03 and 0.61; 6 weeks, 1.40 and 1.10; 8 weeks, 2.02 and 1.46, and control graft recipient mice at 0 weeks, 0; 4 weeks, 0.02 and 0.09; 6 weeks, 0.07 and 0.19; 8 weeks, 0.22 and 0.15. In **f**, data shown are from 1 experiment. (**g**) Analysis of $CD3^+$ cells from pooled spleen and lymph nodes of recipient nude mice 20 weeks post-transplantation. Data shown are representative and are from 1 of 2 independent experiments. WT, wild type. (**h**,**i**) Analysis of IL2 expression in $CD4^+$ cells from lymph nodes of recipient nude mice 20 weeks post-transplantation. Values in **i** represent mean ± s.d. for cells from $n=3$ separate culture dish wells from 1 experiment. Values used to derive mean and s.d. in **i**: wild-type, 55, 33, 75 (unstimulated) and 700, 931, 898 (stimulated); iTEC, 61, 22, 42 (unstimulated) and 572, 403, 780 (stimulated); control, 11, 20, 8 (unstimulated) and 50, 27, 65 (stimulated). See also Supplementary Fig. 5.

T cells were detected in control mice (Fig. 5a–f, Supplementary Fig. 5). These peripheral T cells expressed normal levels of TCRβ and exhibited CD62LCD44 subset phenotypes consistent with the presence of both naive and activated cells (shown for splenocytes in Fig. 5d,e). Analysis of both $CD44^{lo}V\beta^+$ and total $V\beta^+$ cells present in the spleen and lymph node of iTEC-grafted mice indicated a diverse T-cell repertoire (Fig. 5g), the functionality of which was demonstrated by cytokine secretion in response to CD3/CD28 crosslinking (Fig. 5h,i).

The data presented herein establish that enforced expression of FOXN1 is sufficient to convert fibroblasts into iTECs, an *in vitro* generated cell type that exhibits phenotypic and functional properties of *in vivo* TECs. They further show that iTECs are able to promote full T-cell development *in vitro,* potentially offering an improved system for *in vitro* T-cell development over existing models owing to their capacity to express MHC Class II and thus for selection of $CD4^+$ SP thymocytes, a characteristic not observed in other models of *in vitro* T-cell differentiation[36,37]. iTECs thus represent a clear and essential step towards the generation of patient-specific T cells in culture. They further demonstrate that iTECs generate a properly patterned, functional organ on transplantation *in vivo*, composed of cTECs and mTECs that express markers diagnostic of each cell type, including markers critical for T-cell lineage differentiation and repertoire selection. To our knowledge this is the first demonstration of the generation of a complete, organized and functional, complex organ from reprogrammed cells. Our data thus identify iTECs as a new and readily available source of TECs, that may provide the basis for thymus transplantation therapies aimed at boosting adaptive immune system function in immunocompromised patients. □

METHODS

Methods and any associated references are available in the online version of the paper.

Note: Supplementary Information is available in the online version of the paper

ACKNOWLEDGEMENTS

We thank O. Rodrigues and C. Cryer for cell sorting, V. Berno for imaging, F. H. Stenhouse and C. D. Peddie for technical assistance and J. Mee for kidney grafting, R. Zamoyska, R. Brownlie and G. Cowan for advice, V. Wilson, K. Kaji, A. G. Smith, I. Chambers and N. Hastie for comments on the manuscript, and the Biological Research Facility staff for animal care. The research leading to these results received funding from Leukaemia and Lymphoma Research (C.C.B. and N.B.), the Darwin Trust of Edinburgh (S.U.), the School of Biological Sciences, University of Edinburgh (H.J.V.), the Medical Research Council (C.C.B.), the European Union Seventh Framework Programme (FP7/2007–2013) collaborative projects EuroSyStem (C.C.B. and N.B.) and ThymiStem (C.C.B., S.U., K.E.O'N) under grant agreement numbers 200720 and 602587, respectively, and NIH/NIAID grant no. R01 AI082127 (N.R.M.).

AUTHOR CONTRIBUTIONS

N.B. generated the iFoxn1 allele, conceived and designed experiments, performed experiments, analysed the data and contributed to writing the manuscript; N.R.M. contributed to experimental design and to writing the manuscript; S.U., K.E.O'N and H.J.V. performed experiments and contributed to analysis of the data; C.C.B. conceived the original idea, designed experiments, contributed to analysis of the data and wrote the manuscript.

COMPETING FINANCIAL INTERESTS

The authors declare no competing financial interests.

Published online at www.nature.com/doifinder/10.1038/ncb3023
Reprints and permissions information is available online at www.nature.com/reprints

1. Graf, T. & Enver, T. Forcing cells to change lineages. *Nature* **462,** 587–594 (2009).
2. Nehls, M. *et al.* Two genetically separable steps in the differentiation of thymic epithelium. *Science* **272,** 886–889 (1996).
3. Blackburn, C. C. *et al.* The nu gene acts cell-autonomously and is required for differentiation of thymic epithelial progenitors. *Proc. Natl Acad. Sci. USA* **93,** 5742–5746 (1996).
4. Ritter, M. A. & Boyd, R. L. Development in the thymus: It takes two to tango. *Immunol. Today* **14,** 462–469 (1993).
5. Miller, J. F. A. P. Immunological function of the thymus. *Lancet* **2,** 748–749 (1961).
6. Chinn, I. K., Blackburn, C. C., Manley, N. R. & Sempowski, G. D. Changes in primary lymphoid organs with aging. *Semin. Immunol.* **24,** 309–320 (2012).
7. Lynch, H. E. *et al.* Thymic involution and immune reconstitution. *Trends Immunol.* **30,** 366–373 (2009).
8. Manley, N. R., Richie, E. R., Blackburn, C. C., Condie, B. G. & Sage, J. Structure and function of the thymic microenvironment. *Front. Biosci.* **16,** 2461–2477 (2011).
9. Nowell, C. S. *et al.* Foxn1 regulates lineage progression in cortical and medullary thymic epithelial cells but is dispensable for medullary sublineage divergence. *PLoS Genet.* **7,** e1002348 (2011).
10. Bleul, C. C. *et al.* Formation of a functional thymus initiated by a postnatal epithelial progenitor cell. *Nature* **441,** 992–996 (2006).
11. Markert, M. L. *et al.* Transplantation of thymus tissue in complete DiGeorge Syndrome. *N. Engl. J. Med.* **341,** 1180–1189 (1999).
12. Lai, L. & Jin, J. Generation of thymic epithelial cell progenitors by mouse embryonic stem cells. *Stem Cells* **27,** 3012–3020 (2009).
13. Lai, L. *et al.* Mouse embryonic stem cell-derived thymic epithelial cell progenitors enhance T-cell reconstitution after allogeneic bone marrow transplantation. *Blood* **118,** 3410–3418 (2011).
14. Inami, Y. *et al.* Differentiation of induced pluripotent stem cells to thymic epithelial cells by phenotype. *Immunol. Cell Biol.* **89,** 314–321 (2011).
15. Parent, A. V. *et al.* Generation of functional thymic epithelium from human embryonic stem cells that supports host T cell development. *Cell Stem Cell* **13,** 219–229 (2013).
16. Sun, X. *et al.* Directed differentiation of human embryonic stem cells into thymic epithelial progenitor-like cells reconstitutes the thymic microenvironment *in vivo*. *Cell Stem Cell* **13,** 230–236 (2013).
17. Mathis, D. & Benoist, C. Aire. *Annu. Rev. Immunol.* **27,** 287–312 (2009).
18. Klug, D. B. *et al.* Interdependence of cortical thymic epithelial cell differentiation and T-lineage commitment. *Proc. Natl Acad. Sci. USA* **95,** 11822–11827 (1998).
19. Manley, N. R. & Condie, B. G. Transcriptional regulation of thymus organogenesis and thymic epithelial cell differentiation. *Prog. Mol. Biol. Transl. Sci.* **92,** 103–120 (2010).
20. Weiner, L. *et al.* Dedicated epithelial recipient cells determine pigmentation patterns. *Cell* **130,** 932–942 (2007).
21. Allman, D. *et al.* Thymopoiesis independent of common lymphoid progenitors. *Nat. Immunol.* **4,** 168–174 (2003).
22. Klug, D. B., Carter, C., Gimenez-Conti, I. B. & Richie, E. R. Cutting edge: thymocyte-independent and thymocyte-dependent phases of epithelial patterning in the fetal thymus. *J. Immunol.* **169,** 2842–2845 (2002).
23. Revest, J. M., Suniara, R. K., Kerr, K., Owen, J. J. & Dickson, C. Development of the thymus requires signaling through the fibroblast growth factor receptor R2-IIIb. *J. Immunol.* **167,** 1954–1961 (2001).
24. Rubin, J. S. *et al.* Purification and characterization of a newly identified growth factor specific for epithelial cells. *Proc. Natl Acad. Sci. USA* **86,** 802–806 (1989).
25. Adolfsson, J. *et al.* Identification of Flt3+ lympho-myeloid stem cells lacking erythro-megakaryocytic potential. A revised road map for adult blood lineage commitment. *Cell* **121,** 295–306 (2005).
26. Luc, S. *et al.* The earliest thymic T cell progenitors sustain B cell and myeloid lineage potential. *Nat. Immunol.* **13,** 412–419 (2012).
27. Schmitt, T. M. *et al.* Induction of T cell development and establishment of T cell competence from embryonic stem cells differentiated *in vitro*. *Nat. Immunol.* **5,** 410–417 (2004).
28. La Motte-Mohs, R. N., Herer, E. & Zuniga-Pflucker, J. C. Induction of T-cell development from human cord blood hematopoietic stem cells by Delta-like 1 *in vitro*. *Blood* **105,** 1431–1439 (2005).
29. Bennett, A. R. *et al.* Identification and characterization of thymic epithelial progenitor cells. *Immunity* **16,** 803–814 (2002).
30. Sheridan, J. M., Taoudi, S., Medvinsky, A. & Blackburn, C. C. A novel method for the generation of reaggregated organotypic cultures that permits juxtaposition of defined cell populations. *Genesis* **47,** 346–351 (2009).
31. Auerbach, R. Morphogenetic interactions in the development of the mouse thymus gland. *Dev. Biol.* **2,** 271–284 (1960).
32. Jenkinson, W. E., Rossi, S. W., Parnell, S. M., Jenkinson, E. J. & Anderson, G. PDGFRα-expressing mesenchyme regulates thymus growth and the availability of intrathymic niches. *Blood* **109,** 954–960 (2007).
33. Abramson, J., Giraud, M., Benoist, C. & Mathis, D. Aire's partners in the molecular control of immunological tolerance. *Cell* **140,** 123–135 (2010).
34. Shakib, S. *et al.* Checkpoints in the development of thymic cortical epithelial cells. *J. Immunol.* **182,** 130–137 (2009).
35. Murata, S. *et al.* Regulation of CD8+ T cell development by thymus-specific proteasomes. *Science* **316,** 1349–1353 (2007).
36. Schmitt, T. M. & Zuniga-Pflucker, J. C. Induction of T cell development from hematopoietic progenitor cells by delta-like-1 *in vitro*. *Immunity* **17,** 749–756 (2002).
37. Dervovic, D. D. *et al.* Cellular and molecular requirements for the selection of *in vitro*-generated CD8 T cells reveal a role for Notch. *J. Immunol.* **191,** 1704–1715 (2013).
38. Hameyer, D. *et al.* Toxicity of ligand-dependent Cre recombinases and generation of a conditional Cre deleter mouse allowing mosaic recombination in peripheral tissues. *Physiol. Genomics* **31,** 32–41 (2007).
39. Wallace, H. A. *et al.* Manipulating the mouse genome to engineer precise functional syntenic replacements with human sequence. *Cell* **128,** 197–209 (2007).
40. Gray, D. H. *et al.* Unbiased analysis, enrichment and purification of thymic stromal cells. *J. Immunol. Methods* **329,** 56–66 (2008).

METHODS

Ethics statement. All animal work was conducted according to UK Home Office guidelines, as established in the Animals (Scientific Procedures) Act 1986.

Mice. *Rosa26*$^{CAG-STOP-Foxn1-IRES-GFP/+}$ mice were backcrossed onto the C57BL/6 background for at least 5 generations then maintained by intercrossing. *Rosa26*^{CreERt2} (ref. 38) mice were maintained as homozygotes. Six-week- to 6-month-old male *Rosa26*$^{CreERt2/CreERt2}$ mice were crossed with 6–12-week-old *Rosa26*$^{CAG-STOP-Foxn1-IRES-GFP/+}$ female mice as described to generate *Rosa26*$^{CreERt2/CAG-Foxn1-IRES-GFP}$ (iFoxn1) mice. One pregnant iFoxn1 mouse was euthanized to generate each batch of mouse embryonic fibroblasts (MEFs)/iTECs. For timed matings, noon of the day of the vaginal plug was taken as day 0.5.

Generation of the iFoxn1 targeting vector. A construct containing the targeting cassette (Fig. 1a and Supplementary Fig. 1a) was generated by standard molecular biology techniques and verified by sequencing. Conventional subcloning was used for all cloning steps.

Southern blotting. Genomic DNA was processed for Southern blotting as described previously[9].

Gene targeting and blastocyst injection. Mouse Sv129/Ola embryonic stem cells (line E14tg2a) were electroporated with linearized targeting vector (Supplementary Fig. 1a) and grown under geneticin selection. Correctly targeted clones were identified by Southern analysis (Supplementary Fig. 1b), expanded and injected into C57BL/6 blastocysts to generate chimaeric mice. Germ-line transmission was confirmed for two independently targeted cell clones (Supplementary Fig. 1b); the resulting mouse line was designated *Rosa26*$^{CAG-STOP-Foxn1-IRES-GFP/+}$ (called iFoxn1 herein). The neomycin resistance cassette was removed by crossing of founder iFoxn1 mice with Tg(CAG–FLPe) mice[39]. The E14tg2a embryonic stem cell line used to generate the R26-CAG–STOP–Foxn1–IRES–GFP mouse strain is routinely tested for normal karyotype and is tested free of mycoplasma contamination.

MEF isolation. MEFs were prepared from individual E13.5 embryos decapitated and stripped of all internal organs and trypsinized into a single-cell suspension. Cells were plated in DMEM containing 10% fetal calf serum, 2 mM sodium pyruvate, 4 mM glutamine, 50 μg ml^{-1} streptomycin and 50 U ml^{-1} penicillin (DMEM/FCS). Each MEF line was genotyped using the following primers to detect the iFoxn1 allele: iFoxn1F 5′-GGGAGCAGCTGAAGGATGAC-3′ and iFoxn1R 5′-CGCTTGAGGAGAGCCATTTG-3′. *Rosa26*$^{CreERt2/CAG-Foxn1-IRES-GFP}$ (iFoxn1) and *Rosa26*$^{CreERt2/+}$ (Control) MEFs were used for all experiments. MEFs were freshly isolated for each experiment performed in this study.

Tamoxifen treatment. Cells were treated with 1 μ M 4-hydroxy tamoxifen (4OHT; Sigma) for 48 h to induce CreERt2. Control MEFs were exposed to an identical 4OHT treatment.

***In vitro* T-cell development assay.** Five days following 4OHT treatment, 5×10^4 ('low density') or $1–2 \times 10^5$ ('high density') iFoxn1 or control MEFs per well were plated into a 24-well plate. Following a further 2 days, each well was seeded with 3×10^3 DN1 thymocytes (Lin$^-$CD25$^-$c-Kit$^+$) isolated from E14.5 fetal thymi and then co-cultured in DMEM/FCS supplemented with 1 ng ml^{-1} rmIL-7 and 5 ng ml^{-1} rhFlt-3L (PeproTech) for 12 d before analysis. In some experiments 50 ng ml^{-1} rhFGF-7 (PeproTech) was also added to the medium.

***In vitro* T-cell development on OP9-DL1 cells.** OP9-DL1 cells[36] were plated in 24-well plates at 2×10^4 cells per well. Each well was then seeded with 3×10^3 DN1 thymocytes (Lin$^-$CD25$^-$c-kit$^+$) isolated from E14.5 fetal thymi and then co-cultured in a-MEM/FCS supplemented with rhFlt3-3L (Peprotech) at 5 ng ml^{-1} and IL-7 at 5 ng ml^{-1} or 1 ng ml^{-1}. Cultures were monitored daily and non-adherent developing T cells were transferred to a fresh monolayer of OP9-DL1 cells every 3–5 d, when the current layer became confluent. The OP9-DL1 cell line was obtained from K. Kranc (MRC CRM, University of Edinburgh, UK), who had recently obtained it from J. C. Zuniga-Pfluker (University of Toronto, Canada). The line is tested free of mycoplasma contamination.

***In vitro* T-cell stimulation assay.** Cells isolated from the lymph nodes of iTEC or control graft recipient mice were plated into a 96-well plate, pre-coated with CD3 and CD28 (BD Biosciences) (3×10^5 cells per well), and cultured for 24 h before staining for intracellular IL2 (BD Biosciences, clone JES6-5H4).

Grafts. Here, 2×10^5 control or iFoxn1 MEFs (5 days following 4OHT treatment) were mixed with 1×10^5 PDGFR-αβ$^+$ mesenchymal cells and 1×10^5 CD45$^+$Lin$^-$ immature thymocytes isolated from E12.5 to E13.5 fetal thymi, and aggregated for 12–16 h as described[30]. Aggregates were then grafted under the kidney capsule of 6-week-old male CBAxC57BL/6 mice or 5-week-old male nude Foxn1$^{-/-}$ mice (Harlan or Charles River Laboratories). Grafts were removed from CBAxC57BL/6 mice after 4 weeks for immunohistochemical and flow cytometric analyses as described previously[10]. Blood was drawn from the mandibular vein of nude mice after 6 weeks for flow cytometric analyses.

Antibodies. The antibodies used for immunohistochemistry and flow cytometry are listed in Supplementary Table 1. Recipient nude mice were euthanized at various time points after grafting, as described, and spleen and lymph node organs were collected for analysis.

Flow cytometry. For analysis, semi-adherent thymocytes were collected from co-cultures by gentle pipetting; adherent MEFs or iTECs were collected by trypsinization. Adult thymi and recovered graft thymi were enzymatically digested to single-cell suspensions as described previously[40] and processed for cytometric analysis without further enrichment. A TCR Vβ screening panel kit (BD Biosciences) was used to analyse TCR Vβ expression on cells mechanically collected from spleen and lymph nodes of mice. Data were acquired using a LSR Fortessa (BD Biosciences) and analysed using FlowJo software (Tree Star).

For sorting, fetal thymi were enzymatically digested to single-cell suspensions as described previously[9,29]. Total (CD45$^+$Lin$^-$) or DN1 (CD45$^+$Lin$^-$CD25$^-$c-kit$^+$) thymocytes were purified after gating against Lin$^-$ cells (Lin: CD3ϵ, CD4, CD8, CD11b, CD11c, B220, Gr-1, NK1.1, Ter119). Mesenchymal cells (PDGFRαβ$^+$) were purified after gating against CD45$^-$Ter119$^-$ cells. Cell sorting was performed using a FACSAriaII (BD Biosciences).

Immunohistochemistry. Adult thymi and recovered graft thymi were processed for immunohistochemistry as described previously[9]. Isotype controls were included in all experiments. Staining was analysed using a Leica AOBS confocal microscope (Leica Microsystems GmbH). The images presented are either single optical sections or projected focus stacks of serial optical sections.

RNA isolation. RNA was prepared using the RNAeasy mini kit (Qiagen) according to the manufacturer's instructions. All samples were DNase treated.

Quantitative PCR with reverse transcription (RT-qPCR). cDNA was prepared using the Superscript III first strand synthesis kit (Invitrogen) with Oligo-dT primers, according to the manufacturer's instructions. Relative expression levels were determined using the Roche Universal Probe Library on the Roche Lightcycler 480 after normalization to the geometric mean of two housekeeping genes (*Hmbs* and *Tbp*) for all experiments. Technical triplicates were run for all samples and no RT and no template controls were included in all experiments. The primers used for RT-qPCR are listed in Supplementary Table 2. For the analysis presented in Fig. 4d, 50 cells were sorted into CellsDirect 2x Reaction Mix (Invitrogen) supplemented with RNase inhibitor (Ambion). cDNA was synthesized and pre-amplified in a single step using CellsDirect Superscript III reverse transcriptase/Platinum Taq mix (Invitrogen) and gene-specific primers. Thermal cycling conditions were as follows: 50 °C for 15 min; 95 °C for 2 min; 18 cycles of 95 °C for 15 s, 60 °C for 4 min.

Statistical analysis. Statistical analysis was performed using the one-way analysis of variance test (two-tailed), as appropriate for normally distributed data (normal distribution was tested using χ^2 goodness of fit). The α level is taken as 0.05. Errors shown are standard deviations (s.d.) throughout. Sample sizes of at least $n = 3$ were used for statistical analyses except where indicated. No statistical method was used to predetermine sample size, the experiments were not randomized, and the investigators were not blinded to allocation during experiments and outcome assessment. There were no limitations on repeatability of the experiments and no samples were excluded from the analysis.

nature cell biology

DOI: 10.1038/ncb3023

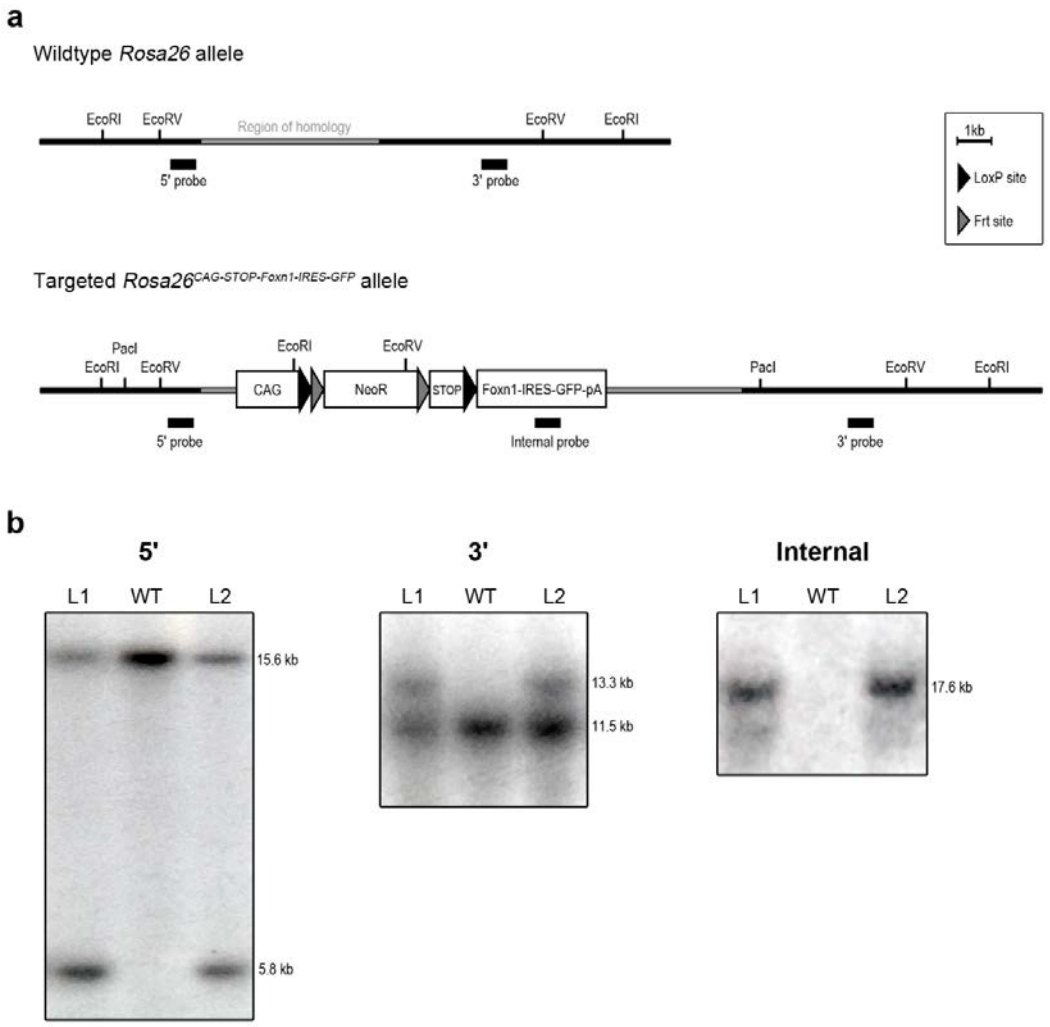

Supplementary Figure 1 related to Figure 1. Generation of transgenic *Rosa26*$^{CAG\text{-}STOP\text{-}Foxn1\text{-}IRES\text{-}GFP}$ mice. **a,** The CAG-STOP-Foxn1 cassette shown in Figure 1 was introduced into the *Rosa26* locus in mouse E14tg2a ES cells by homologous recombination using standard procedures, generating the *Rosa26*$^{CAG\text{-}NeoR\text{-}STOP\text{-}Foxn1\text{-}IRES\text{-}GFP}$ allele. This cassette contained a cDNA encoding Foxn1 under control of the CAG compound promoter and downstream of a LoxP-flanked CMAZ stop cassette plus an IRES-GFP component to permit monitoring of *Foxn1* expression. Neomycin-resistant colonies were picked and screened for targeted insertion by Southern blotting, using the strategy shown in (a) above. The position of restriction enzyme sites and Southern blot hybridization probes are shown for the wild type and transgenic *Rosa26* locus. EcoRI, EcoRV and PacI restriction enzyme digests were used for 5′, 3′ and internal Southern blot analyses, respectively. **b,** Correctly targeted colonies were identified and used to generate chimeric mice via blastocyst injection. Germline transmission was confirmed from two independent ES cell lines (L1 and L2). Founders from each of these *Rosa26*$^{CAG\text{-}NeoR\text{-}STOP\text{-}Foxn1\text{-}IRES\text{-}GFP}$ lines were crossed with *Tg(CAG-FLPe)* mice[39] in order to remove the neomycin resistance cassette (NeoR). These lines were then backcrossed to C57BL/6 mice for five generations before analysis.

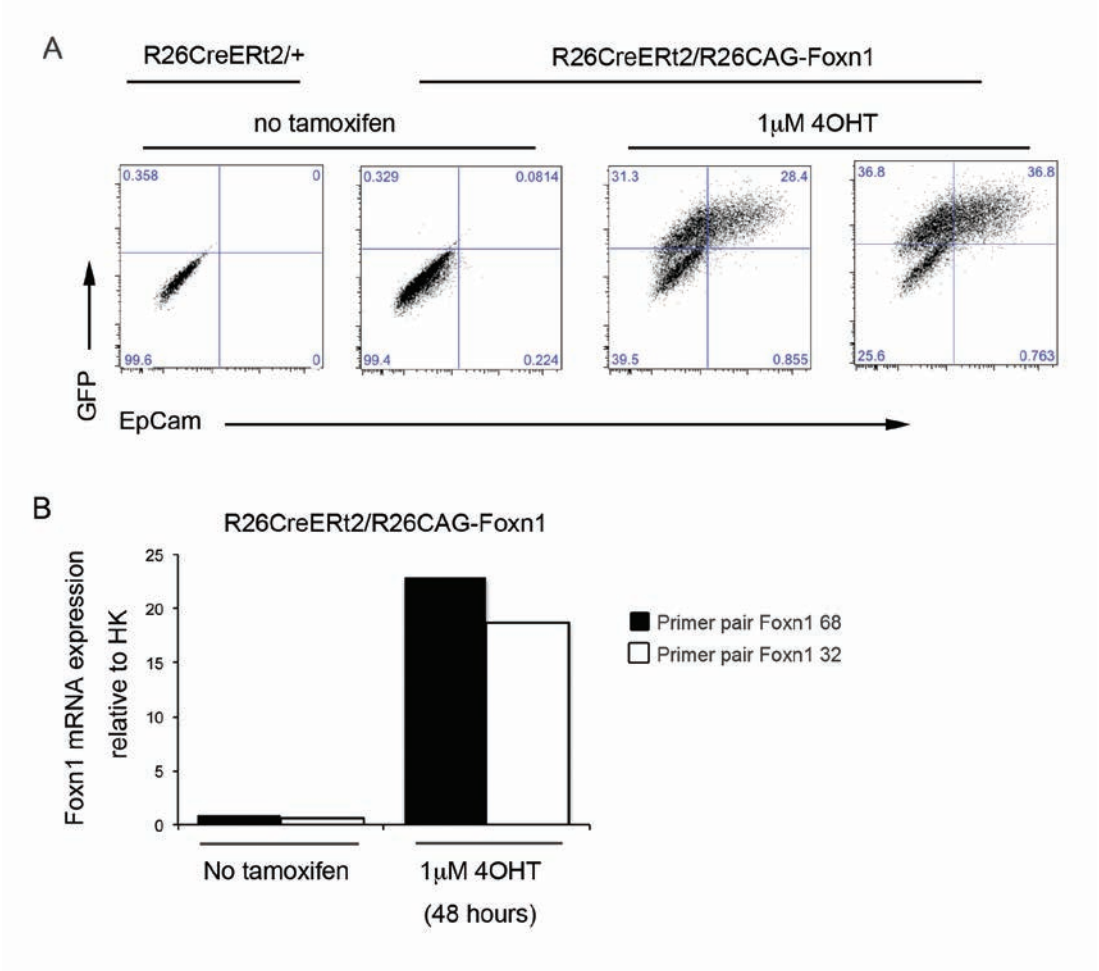

Supplementary Figure 2 related to Figure 1. Absence of tamoxifen-independent Cre-recombinase activity in *Rosa26*$^{CAG\text{-}STOP\text{-}Foxn1\text{-}IRES\text{-}GFP}$ MEFs. MEFs of the genotypes shown were isolated and treated with 1μM 4OHT or carrier solution for 48 hours, then (**A**) analyzed by flow cytometry for expression of GFP and EpCam after a further 4 days in culture, or (**B**) analyzed for *Foxn1* mRNA expression by RT-qPCR (without further culture). Data in (**B**) show *Foxn1* mRNA expression relative to the geometric mean of 2 housekeepers, determined for two *Foxn1* primer/UPL probe sets, Foxn1 68 and Foxn1 32. No GFP or *Foxn1* expression was detected in the absence of tamoxifen/4OHT, indicating that leakiness caused by ligand-independent Cre-recombinase activity did not occur in this system.

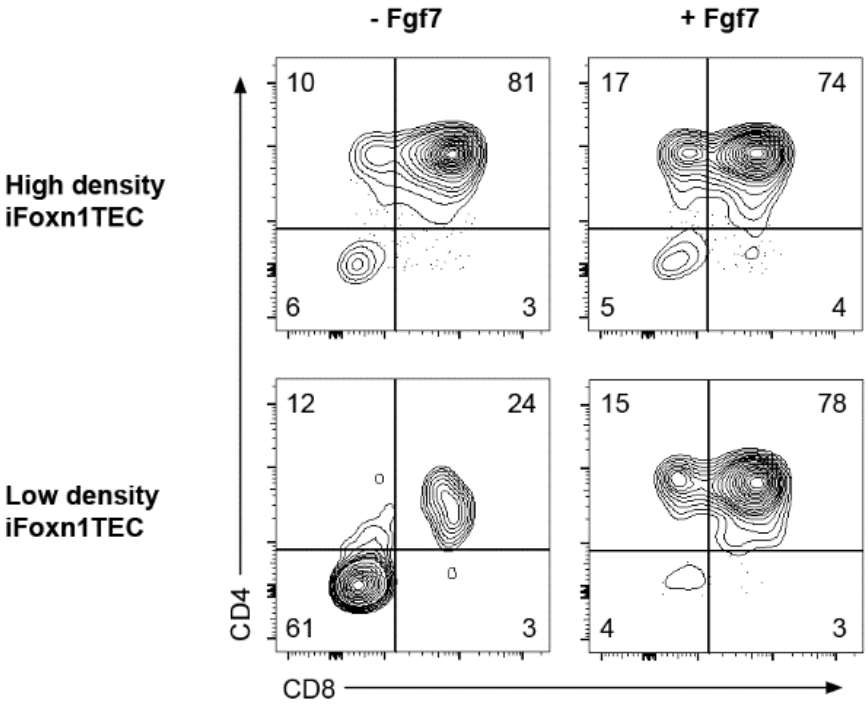

Supplementary Figure 3 related to Figure 2. iFoxn1TEC are responsive to Fgf7 *in vitro.* Plots show flow cytometric analysis of $CD45^+$ cells following co-culture on iTEC for 12 days in the presence or absence of Fgf7. iTEC (five days after induction of Foxn1) were plated at low density ($5x10^4$ cells per well) or high density ($2x10^5$ cells per well) into a 24-well plate. Following a further 2 days each well was seeded with $3x10^3$ ETP thymocytes ($CD45^+Lin^-CD25^-C\text{-}Kit^+$) isolated from E14.5 fetal thymi and cultured for 12 days before analysis.

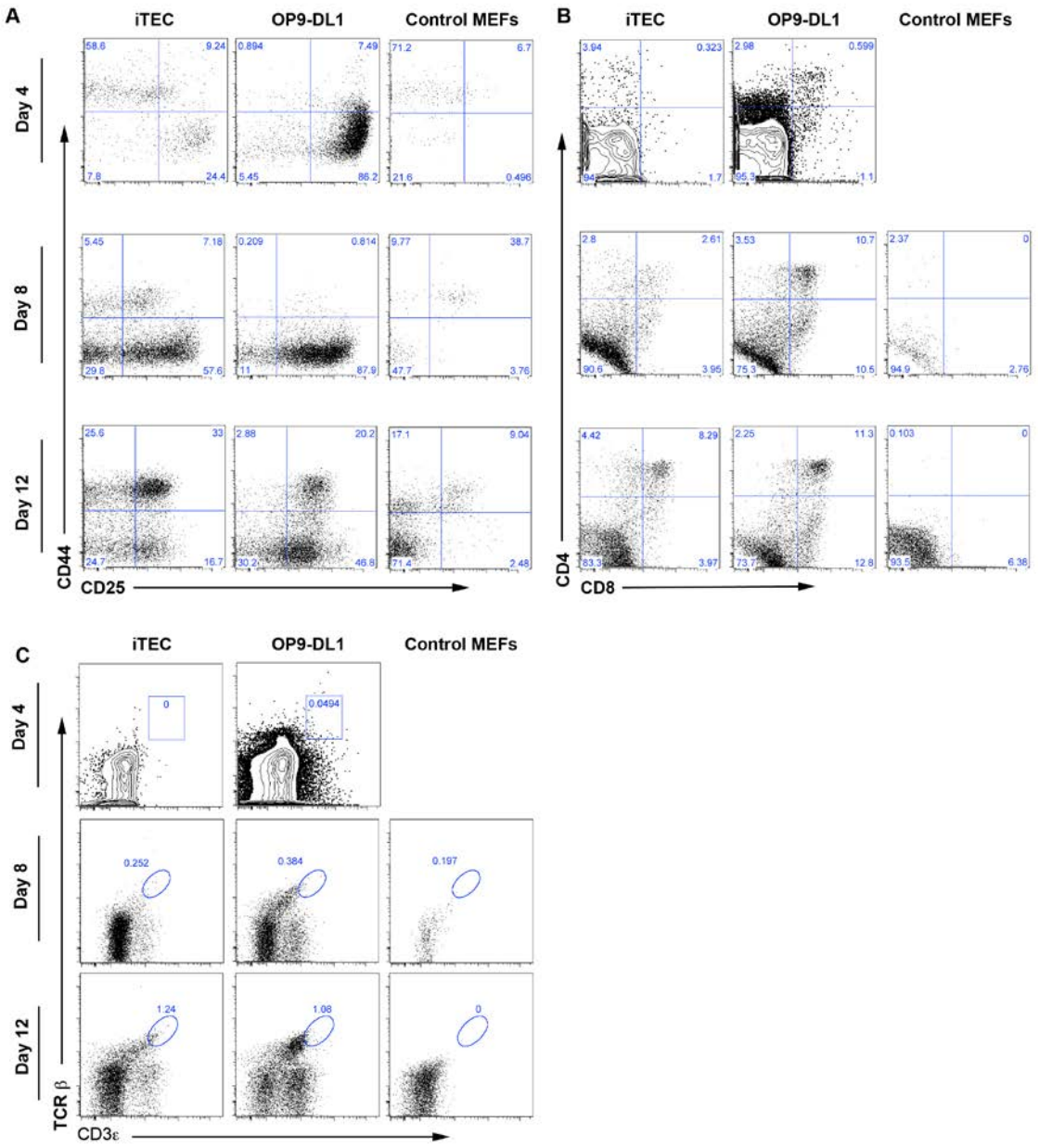

Supplementary Figure 4 related to Fig. 2. Comparison of the kinetics of T cell development in vitro from ETP seeded onto iTEC or OP9-DL1 cells. ETP were isolated from E14.5 fetal thymi and seeded at a density of 3000 cells per well onto OP9-DL1 cells (plated the previous day at a density of $2x10^4$ per well) or iTEC (density $2x10^5$) in 24 well plates. The OP9-DL1/ETP co-cultures were subsequently cultured in medium containing IL7 (5ng/ml) and Flt3L (5ng/ml) (Porrit et al., 2004) until day 6 of culture, then IL7 (1ng/ml) and Flt3L (5ng/ml) until the end of the experiment, while the iTEC/ETP and control MEF/ETP co-cultures were cultured in medium containing IL7 (1ng/ml) and Flt3L (5ng/ml) throughout. Cultures were analyzed by flow cytometry with the markers shown after 4, 8 or 12 days of co-culture. n=1.

Note that the iTEC used for the above experiments were made by isolating MEFs from E13.5 *Rosa26*$^{CAG\text{-}STOP\text{-}Foxn1\text{-}IRES\text{-}GFP}$ embryos; these MEFs were expanded in culture for 4 days, then treated with 1μM 4OHT for 48 hours. The following day, GFP$^+$ cells were isolated by flow cytometric cell sorting, then plated into 24 well plates at a density of $2x10^5$ cells per well. They were seeded with ETPs 3 days later. This protocol differs slightly from the protocol used in Figure 2.

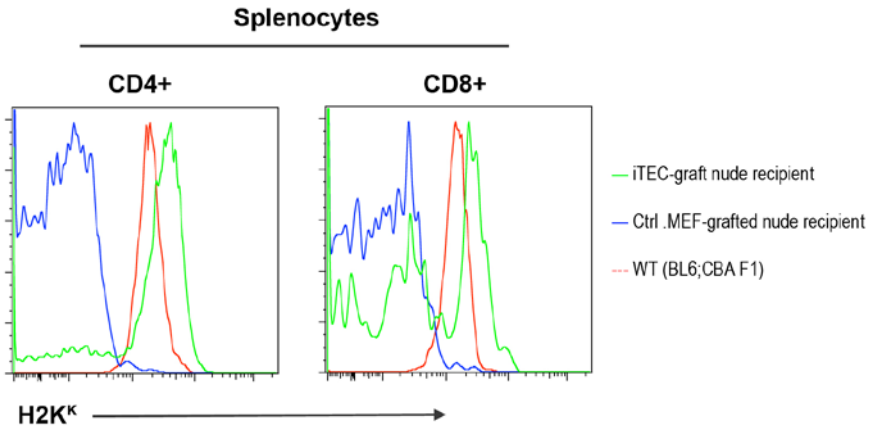

Supplementary Figure 5 related to Fig. 5. Haplotype analysis demonstrates the presence of donor-derived T cells in iTEC-graft recipients. Representative analysis of splenocytes from iTEC-grafted or control-grafted *nu/nu* mice seven weeks post-transplantation, and wild type (WT) C57BL/6xCBA F1 mice. Plots show staining for H2K^{k} on CD4^{+} and CD8^{+} splenocytes after gating on live cells. The donor ETP within the iTEC and control grafts were from C57BL/6xCBA F1 embryos and therefore expressed b and k haplotypes of MHC Class I and II antigens. The recipient mice were CD1 *nu/nu*, which are of undetermined haplotype, but do not express H2Kk as shown. Most splenic T cells in the iTEC recipients are donor-derived (i.e. express H2K^{k}).

Supplementary Table 1. Antibodies used for immunofluorescence and flow cytometry. FC, flow cytometry; IF, immunofluorescence

Antibody	Clone	Supplier	Dilution	Staining
Aire (M-300)	Polyclonal	SCBT	1/300	IF
B220 FITC	RA3-6B2	BioLegend	1/200	FC – Lineage (DN sort), T cell analysis
Beta5t	Polyclonal	MBL International	1/200	IF
CD11b FITC	M1/70	E-Bioscience	1/200	FC – Lineage (DN sort)
CD11c FITC	N418	E-Bioscience	1/200	FC – Lineage (DN sort)
CD205	NLDC-145	AbD Serotec	1/10	IF
CD25 PE	PC61	BioLegend	1/100	FC – DN1 sort
CD3e FITC	145-2C11	E-Bioscience	1/200	FC – Lineage (DN sort)
CD3e PE	145-2C11	BioLegend	1/200	FC – T cell analysis
CD4 FITC	RM4-5	BD Biosciences	1/200	FC – Lineage (DN sort), T cell analysis
CD4 PE-Cy7	RM4-5	E-Bioscience	1/400	FC – T cell analysis
CD45 APC	30-F11	E-Bioscience	1/200	FC – DN1 sort, T cell analysis
CD45 APC-eFluor780	30-F11	E-Biosciences	1/200	FC – T cell analysis
CD45 PerCP-Cy5.5	30-F11	E-Biosciences	1/200	FC – DN/mesenchyme sort, graft analysis
CD8a APC	53-6.7	E-Bioscience	1/200	FC – T cell analysis
CD8a FITC	53-6.7	E-Bioscience	1/200	FC – Lineage (DN sort)
CD8a PE	53-6.7	E-Bioscience	1/200	FC – T cell analysis
C-Kit APC-eFluor780	2B8	E-Bioscience	1/100	FC – DN1 sort
Cytokeratin 14 (AF 64)	Polyclonal	Covance	1/800	IF
Cytokeratin 8	Troma1	DSHB	1/10	IF
DAPI (4',6-Diamidino-2-Phenylindole, Dihydrochloride)	Life Technologies	Invitrogen	0.5ug/ml (FC); 5ug/ml (IF)	Viability dye
EpCAM APC	G8.8	BioLegend	1/400	FC – MEF/graft analysis
Foxp3 A488	MF-14	BioLegend	Manufacturer's instructions	FC – T cell analysis
Gr-1 FITC	RB6-8C5	E-Bioscience	1/200	FC – Lineage (DN sort)
IL-2	JES6-5H4	BD Biosciences	1/200	FC
MHC Class II PE-Cy7	M5/114.15.2	BioLegend	1/800	FC – MEF/graft analysis
NK1.1 FITC	PK136	BD Biosciences	1/200	FC – Lineage (DN sort)
Pan-Cytokeratin	Polyclonal	DAKO	1/800	IF
PDGFR-a APC	APA5	BioLegend	1/200	FC – Mesenchyme sort
PDGFR-b APC	APB5	BioLegend	1/200	FC – Mesenchyme sort
TCRb PerCP-Cy5.5	H57-597	BioLegend	1/200	FC – T cell analysis
TCRgd FITC	GL3	BioLegend	1/200	FC – T cell analysis
Ter119 FITC	Ter119	E-Bioscience	1/200	FC – Lineage (DN sort)
UEA-1 biotin	Lectin	Vector Labs	1/400	IF

Supplementary Table 2. Primers used for RT-PCR

Gene	Forward primer (5′-3′)	Reverse primer (5′-3′)
CCL25	GAGTGCCACCCTAGGTCATC	CCAGCTGGTGCTTACTCTGA
CD205	CTCACGTGGCTATGCAAGAG	GGATGGCTATGCCTGTGTAGT
CTSL	CAAATAAGAATAAATATTGGCTTGTCA	TCGTCTTTCACAAGTGTCTTCAG
CXCL12	GGTTCTTCGAGAGCCACA TC	TGTTCTTCAGCCGTGCAA
Dll4	AGGTGCCACTTCGGTTACAC	GGGAGAGCAAATGGCTGATA
EVA	TGTGCTTCCACTTCTCCTGA	TCCACAGCTTCTGTAGGACAAA
Fgf2	CGGCTCTACTGCAAGAACG	TGCTTGGAGTTGTAGTTTGACG
FgfR2IIIB	CGGGGTGTTGGAGTTCA T	CCTGCGGAGACAGGTAACA
Foxn1 32	CTCTCACTGACTTCGACTTCCA	CGACGAGGTCACCAATACG
Foxn1 68	TGACGGAGCACTTCCCTTAC	GACAGGTTATGGCGAACAGAA
Foxn1-3'UTR	CTTAAAGGTCAAAGAAGGAAAACACT	GGCTAACAAATAAGTTGGCTGAG
HMBS	TCCCTGAAGGATGTGCCTAC	ACAAGGGTTTTCCCGTTTG
Keratin 1	CCAGGTGCTACAAACCAAATG	GTTTTGGGTCCGGGTTGT
Kit L	TCAACATTAGGTCCCGAGAAA	ACTGCTACTGCTGTCATTCCTAAG
P63	GGAAAACAATGCCCAGACTC	AATCTGCTGGTCCATGCTGT
Pax9	AGCAGGAAGCCAAGTACGG	TGGATGCTGAGACGAAACTG
TBP	GGGGAGCTGTGATGTGAAGT	CCAGGAAATAATTCTGGCTCA